

Enhanced optical field intensity distribution in organic photovoltaic devices using external coatings

Brendan O'Connor, Kwang H. An, and Kevin P. Pipe^{a)}

Department of Mechanical Engineering, The University of Michigan, Ann Arbor, Michigan 48109-2125

Yiyang Zhao and Max Shtein^{b)}

Department of Material Science and Engineering, The University of Michigan, Ann Arbor, Michigan 48109-2125

(Received 7 August 2006; accepted 23 October 2006; published online 4 December 2006)

An external dielectric coating is shown to enhance energy conversion in an organic photovoltaic cell with metal anode and cathode by increasing the optical field intensity in the organic layers. Improved light incoupling in the device is modeled using transfer matrix simulations and is confirmed by *in situ* measurement of the photocurrent during growth of the coating. The optical field intensity in optimized cell geometries is predicted to exceed that in analogous devices using indium tin oxide, both cell types having equivalent anode sheet resistance, suggesting a broader range of compatible substrates (e.g., metal foils) and device processing techniques. © 2006 American Institute of Physics. [DOI: 10.1063/1.2399937]

An archetypal heterojunction organic photovoltaic (PV) cell consists of light-absorbing organic thin films sandwiched between two electrodes, where at least one electrode is transparent.¹ Photocurrent generation in this device proceeds via a multistep process, the overall efficiency of which is in part limited by the trade-off between efficient optical absorption and exciton diffusion to the electron donor-acceptor (D-A) interface, where charge dissociation occurs.² This limitation is thought to originate from the short exciton diffusion length relative to the optical absorption length in compounds typically employed in organic PV cells.² For a flat heterojunction structure, an optimal balance between light absorption and exciton diffusion is achieved for thin (on the order of 500 Å) organic layers. This, however, places one of the organic layers (e.g., electron acceptor) close to the optically thick metallic electrode (e.g., cathode), where the electromagnetic field vanishes, thereby reducing the net rate of exciton generation near the D-A interface.^{3,4}

Several approaches to simultaneously improve light absorption and exciton diffusion have been investigated, including the use of materials with longer exciton diffusion lengths,⁵ bulk heterojunction morphologies,⁶⁻⁸ exciton-blocking layers (EBLs),⁹⁻¹¹ light trapping,⁹ and sensitizing layers.¹² In these approaches, however, the optical field intensity near the D-A interface cannot be controlled independently of the electrical properties of the active organic layers that are sandwiched between the electrodes.

Here we model and experimentally demonstrate a device structure incorporating *external* dielectric layers that allow for the increase in the optical field intensity at the D-A interface, and hence the exciton generation rate, independently of the active organic layer structure. The capping layer is similar in its optical function to conventional antireflection coatings used in optics,¹³ yet it differs in that it tunes the phase of the incoming radiation to maximize the field intensity near the donor-acceptor interface that is unique to thin film organic PV devices. The coating can also serve the role of a

barrier layer to protect the PV cell from the ambient.

Compare an archetypal organic PV cell structure shown in Fig. 1(a) to an alternative structure illustrated in Fig. 1(b). In the latter, a thick metal anode replaces indium tin oxide (ITO), while the cathode is comprised of a semitransparent aluminum and silver film, followed by a dielectric cap; light enters the cell through the cathode. A similar structure was used previously to increase the light extraction efficiency in top emitting organic light emitting devices.¹⁴ Here, we calculate the optical field intensity profile for the layer structures in Fig. 1 using the transfer matrix method,^{2,15} assuming monochromatic light propagating normal to the device layers and typical optical constants for the active organic layers and organic dielectric cap.^{15,16} The calculated field intensity profiles are superimposed onto the structures in Fig. 1, being

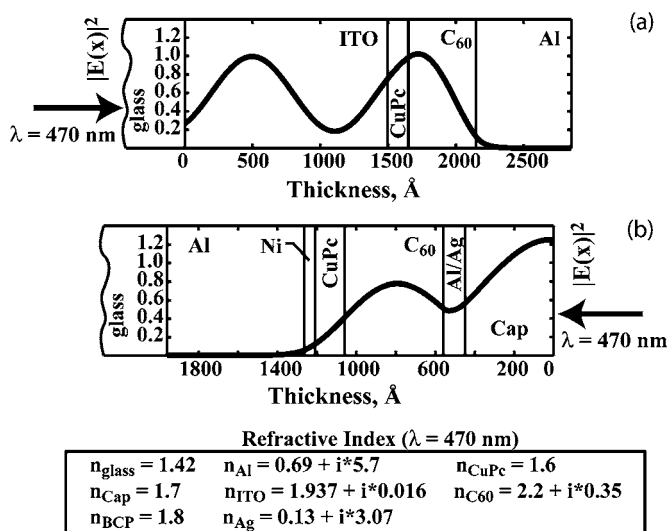


FIG. 1. Schematics of (a) an archetypal organic photovoltaic device that uses an ITO anode on a glass substrate and (b) an alternative device structure with metal anode and cathode, capped by a 450 Å thick dielectric layer having a refractive index n_{cap} of 1.7. Superimposed is the normalized electric field component of the optical field intensity $|E_{\text{DA}}|^2$ throughout the structure, calculated using a thin film transfer matrix model. In the structure in (a), $|E_{\text{DA}}|^2 = 0.98$. In the structure in (b), $|E_{\text{DA}}|^2 = 0.41$.

^{a)}Electronic mail: pipe@umich.edu

^{b)}Electronic mail: mshtein@umich.edu

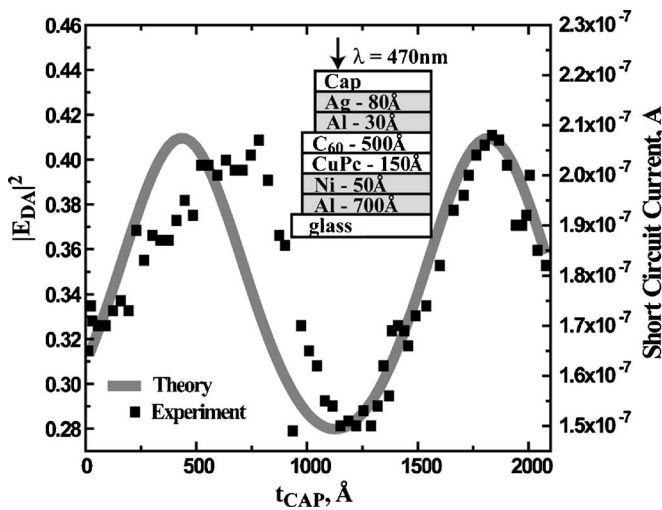


FIG. 2. Plot of the calculated value of $|E_{DA}|^2$ vs the dielectric capping layer thickness t_{cap} in the device structure shown in the inset (solid line), predicting an increase of up to 31% in $|E_{DA}|^2$ when a capping layer is introduced. Superimposed are the data points corresponding to the short-circuit photocurrent J_{SC} measured *in situ* during the growth of the capping layer under constant illumination at 470 nm, showing an increase in the photocurrent and, hence, the power conversion efficiency compared to the uncapped device.

normalized to the incident free-space optical field intensity. Of interest in this discussion is the normalized electrical field intensity at the D-A interface, $|E_{DA}|^2$.

The detailed structure used in the first simulation is shown in the inset of Fig. 2, and consists of 1 mm glass substrate, 700 Å of aluminum (Al), 50 Å of nickel (Ni), 150 Å of copper phthalocyanine (CuPc), 500 Å of C_{60} , 30 Å of Al, 80 Å of silver (Ag), and a capping layer (cap) of varying thickness. If no absorption or photon downconversion takes place in the capping layer, $|E_{DA}|^2$ will vary periodically with the capping layer thickness (t_{cap}) due to optical interference effects, as shown in Fig. 2. Note that $|E_{DA}|^2$ for a capping layer thickness of 470 Å is approximately 30% higher than in the device without the capping layer, suggesting that a similar increase in the photocurrent and conversion efficiency can be expected.

To verify this prediction, we measured the photocurrent produced by a PV cell with this structure during the deposition of the capping layer. Here the organic PV cell layers were grown at 10^{-6} Torr at deposition rates of 2 and 1 Å/s for the organic and metal layers, respectively. The capping layer consisted of aluminum hydroxyquinoline (Alq_3) deposited at an average rate of 3 Å/s; Alq_3 was chosen primarily for convenience of deposition and its weak overlap of absorption with that of the CuPc/ C_{60} stack.¹⁷ The illumination source was a blue InGaN light emitting diode with a peak wavelength of 470 nm and a spectral half width of 25 nm. The excitation wavelength corresponds to the peak absorption of C_{60} within the visible portion of the spectrum.¹⁵ The current-voltage response of the PV cell was obtained using an Agilent 4156B semiconductor parameter analyzer by scanning the voltage from -0.2 to 0.7 V at 20 s intervals.

The measured short-circuit current is plotted versus t_{cap} in Fig. 2, superimposed on the plot of the calculated $|E_{DA}|^2$. Indeed the measured photocurrent closely follows the predicted $|E_{DA}|^2$ curve, confirming the linear dependence of photocurrent on intensity near the D-A interface, and a 30% increase in the photocurrent compared to the uncapped de-

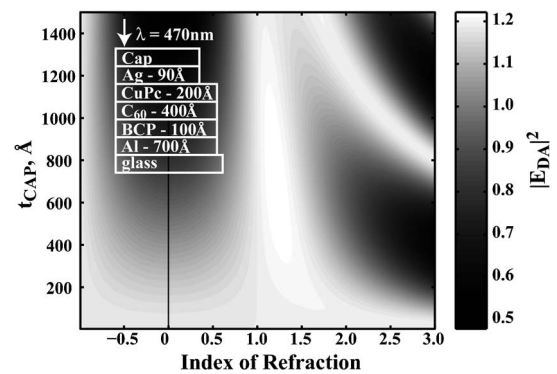


FIG. 3. Gray-scale map of the $|E_{DA}|^2$ values in a high efficiency heterojunction organic photovoltaic device incorporating an exciton-blocking layer (EBL), whose structure is shown in the inset, vs the thickness and index of refraction of the dielectric capping layer. The plot was obtained from a thin film transfer matrix calculation for incident light having 470 nm wavelength. The maximum $|E_{DA}|^2$ is 1.22, normalized by the free-space value, for a cap thickness of 720 Å and $n_{cap}=1.2$. For a similar device structure with a 1500 Å ITO anode, $|E_{DA}|^2$ is 1.04. While an index of refraction as low as 1.2 is not common, similar enhancement can be attained using $n > 1.7$, as well as multiple-layer configurations where the layers have more typical values of n .

vice. It is also noted that the integrated field intensity over the C_{60} layer has a periodic behavior similar to $|E_{DA}|^2$, which is expected due to the long diffusion length L_D of excitons in C_{60} .⁵ Nevertheless, for many organic PV materials and structures which have shorter L_D , $|E_{DA}|^2$ remains a key design principle for optimization. The observed small discrepancy between the phases of the experimental data and theoretical prediction for small values of t_{cap} may be attributed to the deposited film morphology, which is not taken into account by the simulation.

To estimate the extent to which this approach can increase the efficiency of organic PV devices, we now extend our model to predict $|E_{DA}|^2$ for an archetypal heterojunction cell that includes an EBL. The proposed device structure is shown in the inset of Fig. 3. It includes a 90 Å thick silver anode, which is predicted to have a sheet resistance equivalent to a typical ITO layer thickness of 1500 Å.^{18,19} For illumination at a single wavelength of 470 nm, the simulation predicts that the thickness and refractive index of the capping layer can be chosen such that the value of $|E_{DA}|^2$ in the device with metallic anode and cathode can exceed that in an analogous device that employs an ITO anode. We note that multiple combinations of t_{cap} and refractive index n_{cap} are possible, including those with $n_{cap} \approx 1.2$ and $n_{cap} > 1.7$. In the case examined here, the maximum $|E_{DA}|^2$ is 1.22, normalized by the free-space value, for a cap thickness of 720 Å and $n_{cap}=1.2$; $n_{cap} > 1.7$ can yield comparable enhancement. While an index of 1.2 is not common, similar enhancement can be attained using dielectrics with higher values of the refractive index, as well as multiple-layer configurations in which the layers have more typical values of n . The approach described in this work can be extrapolated to design multilayer coatings that improve PV cell performance for broad band and oblique illuminations, as has been shown previously for dielectric mirrors and antireflective coatings.^{13,20}

In conclusion, we have shown that an external dielectric coating can be designed to substantially improve the light in coupling efficiency in an organic photovoltaic (PV) cell, especially if both electrodes are metallic. The theoretical pre-

diction was verified by *in situ* measurements of the photocurrent during growth of the capping layer. The ability to replace ITO coatings by thin metal films potentially improves the overall mechanical properties²¹ of the devices and can lower the cost of substrates. Furthermore, the ability to couple light in through the top-deposited cathode allows for a wider range of organic PV cell designs, including devices deposited directly onto opaque substrates (e.g., metal foil).

The authors would like to thank Peter Burgardt and the Kotov group at the University of Michigan for their assistance with this work, the Office of Naval Research Contract No. N00014-05-1-0713, the National Science foundation ECS-0523986, and the Air Force Office of Scientific research Contract No. FA9550-06-1-0399 for the financial support of this work.

¹C. W. Tang, Appl. Phys. Lett. **48**, 183 (1986).

²P. Peumans, A. Yakimov, and S. R. Forrest, J. Appl. Phys. **93**, 3693 (2003).

³S. R. Forrest, MRS Bull. **30**, 28 (2005).

⁴H. Hoppe and N. S. Sariciftci, J. Mater. Res. **19**, 1924 (2004).

⁵Y. Shao and Y. Yang, Adv. Mater. (Weinheim, Ger.) **17**, 2841 (2005).

⁶P. Peumans, S. Uchida, and S. R. Forrest, Nature (London) **425**, 158 (2003).

⁷G. Li, V. Shrotriya, J. S. Huang, Y. Yao, T. Moriarty, K. Emery, and Y. Yang, Nat. Mater. **4**, 864 (2005).

⁸K. M. Coakley and M. D. McGehee, Chem. Mater. **16**, 4533 (2004).

⁹P. Peumans, V. Bulovic, and S. R. Forrest, Appl. Phys. Lett. **76**, 2650 (2000).

¹⁰B. P. Rand, J. Li, J. G. Xue, R. J. Holmes, M. E. Thompson, and S. R. Forrest, Adv. Mater. (Weinheim, Ger.) **17**, 2714 (2005).

¹¹J. Y. Kim, S. H. Kim, H. H. Lee, K. Lee, W. L. Ma, X. Gong, and A. J. Heeger, Adv. Mater. (Weinheim, Ger.) **18**, 572 (2006).

¹²K. Ishikawa, C. J. Wen, K. Yamada, and T. Okubo, J. Chem. Eng. Jpn. **37**, 645 (2004).

¹³Jenny Nelson, *The Physics of Solar Cells* (Imperial College Press, London, 2003), Vol. 1, p. 363.

¹⁴H. Riel, S. Karg, T. Beierlein, B. Ruhstaller, and W. Riess, Appl. Phys. Lett. **82**, 466 (2003).

¹⁵L. A. A. Pettersson, L. S. Roman, and O. Inganäs, J. Appl. Phys. **86**, 487 (1999).

¹⁶B. P. Rand, P. Peumans, and S. R. Forrest, J. Appl. Phys. **96**, 7519 (2004).

¹⁷I. Sokolik, R. Priestley, A. D. Walser, R. Dorsinville, and C. W. Teng, Appl. Phys. Lett. **69**, 4168 (1996).

¹⁸W. Zhang, S. H. Brongersma, O. Richard, B. Brijs, R. Palmans, L. Froyen, and K. Maex, Microelectron. Eng. **76**, 146 (2004).

¹⁹A. F. Mayadas, M. Shatzkes, and J. F. Janak, Appl. Phys. Lett. **14**, 345 (1969).

²⁰M. Deopura, C. K. Ullal, B. Temelkuran, and Y. Fink, Opt. Lett. **26**, 1197 (2001).

²¹D. R. Cairns and G. P. Crawford, Proc. IEEE **93**, 1451 (2005).